energies

MDPI

*Article*

# Analysis of the Influence Factors of the Crude Oil Temperature Maintenance System of Solar Sewage Heat Pumps in Cold Regions

**Shangwen Zhu [1], Xiaohua Gu [1,2,*], Mengyi Duan [1], Feiyang Yu [1], Danyi Zhao [1], Siwen Liu [3] and Yan Liu [1,*]**

1 School of Energy and Building Environment, Guilin University of Aerospace Technology, Guilin 541004, China; glzsw2337899@163.com (S.Z.); 15517977333@163.com (M.D.); 17773084776@163.com (F.Y.); zdy20020326@163.com (D.Z.)

2 State Key Laboratory for Modification of Chemical Fibers and Polymer Materials, College of Materials Science and Engineering, Donghua University, Shanghai 200051, China

3 College of Innovative Material & Energy, Hubei University, Wuhan 430062, China; 202121113012770@stu.hubu.edu.cn

* Correspondence: 2022043@guat.edu.cn (X.G.); 2019009@guat.edu.cn (Y.L.); Tel.: +86-18121138868 (X.G.); +86-18078343019 (Y.L.)

**Abstract:** Traditional crude oil heating methods that use fossil fuels or electricity have the disadvantages of high consumption of nonrenewable resources, low energy utilization, and high carbon emissions. Therefore, it is urgent to develop green and sustainable crude oil heating technologies. In this paper, a solar synergistic sewage heat pump (SSHS) dual heat source crude oil temperature maintenance system is proposed. The system utilizes clean and sustainable solar energy to heat crude oil while combining sensible heat storage technology and the waste heat utilization technology of a sewage source heat pump to solve the unstable fluctuation of the solar heating problem. A simulation and analysis model is established to analyze the influencing factors of the SSHS, and the optimal operation scheme is provided. The results show that the efficiency of the solar collector decreases and the proportion of crude oil heating increases with an increase in the solar energy guarantee rate, while the unit flow rate of the pump has a large impact on the performance of the sewage source heat pump. In order to avoid energy waste, it is more appropriate to adopt a 30% guarantee rate and an A3 pump unit flow rate, under which the solar collector efficiency is 50.18%, the proportion of solar heating of crude oil is 47.16%, the average temperature of crude oil is 42.59 °C, and the COP of the sewage source heat pump is 4.65. Further increases in the COP of the wastewater source heat pump can be realized by increasing the temperature of the wastewater supply. The results of this study provide a valuable reference for the optimization of crude oil storage heating systems.

**Keywords:** solar energy; sewage source heat pump; crude oil; TRNSYS; system operating characteristics



**Citation:** Zhu, S.; Gu, X.; Duan, M.; Yu, F.; Zhao, D.; Liu, S.; Liu, Y. Analysis of the Influence Factors of the Crude Oil Temperature Maintenance System of Solar Sewage Heat Pumps in Cold Regions. *Energies* **2023**, *16*, 8124. https://doi.org/10.3390/en16248124

Academic Editor: Philippe Leclère

Received: 13 November 2023
Revised: 13 December 2023
Accepted: 17 December 2023
Published: 18 December 2023



## 1. Introduction

With the rapid development of the economy and technology, the demand for crude oil as an essential building block for development has been increasing annually [1]. This sustained growth in demand for crude oil has prompted, for safety and security, the control of oil reserves to become a concern for global economic development. Large floating roof tanks have become important examples of oil storage equipment due to their structural and economic advantages [2]. At the same time, the global crude oil production regions are widespread and span a large area, with some oil fields being located in severely cold regions [3].

In cold regions, the temperature of the crude oil stored in large floating roof oil tanks gradually decreases through the tank roof, tank wall, and tank bottom soil to the outside world and via heat dissipation [4,5]. When the temperature of crude oil falls to freezing point, the crude oil undergoes the gelation phenomenon and gelatinized crude oil is attached to the edge of the tank body of the large floating roof tanks, thus forming a certain thickness of a solid condensate layer [6,7]. This results in increased flow resistance and even the accumulation of condensate, which blocks the import and export of the oil, thus affecting the delivery and receipt of the oil and other turnover operations.

Crude oil heating [8,9] is a necessary measure through which to prevent accidents during the storage and transportation of crude oil in large floating roof tanks. However, traditional boiler heating and electric heating have problems such as high energy consumption and carbon emissions, and air source heat pumps [10] and ground source heat pump [11] heating have limitations in the use of the environment; as such, the development of a new type of heat source supply is imminent. Solar energy [12,13] is a green and low-carbon energy source, and the utilization of solar energy as a heat source for maintaining the temperature of crude oil in large floating roof tanks can reduce primary energy consumption, greenhouse gas emissions, and environmental pollution. Notably, in China's oil-rich Heilongjiang and Neimenggu (which, respectively, belong to cold regions), there are abundant solar energy resources for the development of floating roof oil tanks, solar phase-change heat storage, and thermoregulation technology. Previous research on solar collectors has focused on their application in industrial production processes, and relatively little research has been carried out on the potential of solar energy in heating crude oil. However, its methodology can provide theoretical guidance for this study.

In the field of solar energy industrial applications, previous research efforts [14,15] have begun to explore its potential applications in depth. Mohammadi et al. [16] conducted a comprehensive technical and economic analysis for a solar industrial process heat (SIPH) plant in Salt Lake City, Utah. The results showed that the use of parabolic trough collectors can significantly reduce operating costs and greenhouse gas emissions compared to conventional natural, gas-fired power plants. On the other hand, certain scholars [17,18] have optimized the design of a solar industrial heating system to significantly reduce the annual lifecycle cost in order to generate a low-to-medium process heat so as to meet the heat demand of the industrial process while minimizing the dependence on fossil fuels.

As far as the solar heating of crude oil is concerned, researchers such as Wang [19] assessed the potential for applying solar energy in the global oil business via covering a wide range of segments such as extraction, transportation, and refining. It was found that the potential demand for solar photovoltaic (PV) and solar thermal power in this sector ranges from 17 to 95 gigawatts (GW) and 21 to 95 GW, respectively. These estimates clearly reveal the huge future demand for solar energy in the oil and gas industry. The demand for solar energy from the oil and gas industry is expected to continue to rise over the next two decades. It is predicted that solar energy will contribute about 2 quintillion joules (PJ) to the industry by 2035, which is about 5% of the overall industry's energy demand [20]. Altayib et al. [21] used a solar heating system to replace 10% of the heat required for preheating crude oil before processing. The overall energy efficiency and power generation efficiency of the system reached 60.94% and 19.34%, respectively. It was also found that the solar unit and heat exchanger were the major components contributing to the energy consumption in the system. Naseer Ahmad Khan et al. [22] simulated the solar synergistic TES heating system for the heating of crude oil through transient simulation, and the results of the study showed that it could provide a cost saving of USD 21.046 million over the maximum lifecycle and 116,944 MWh of heat per year; additionally, GHG emissions could be reduced by approximately 34.045 tons of $CO_2$ equivalent per year.

In the field of crude oil storage, the application of solar energy is different from other industrial sectors. This is due to the fact that the demand for thermal energy was continuous during the period of static storages of crude oil. Therefore, solar heating systems have the potential to meet thermal energy demand during crude oil storage under conditions of continuous and sufficient solar radiation. However, the intensity of solar radiation is characterized by periodic fluctuations due to natural factors such as the climate, geography, weather, and diurnal variations [21]. This leads to the possibility of overheating or underheating of the heating temperature of the solar heating system.

In order to solve this problem, the main methods include the use of solar photovoltaic technology combined with thermal storage [23], or the utilization of other heating technologies [24,25]. By these means, the temperature of crude oil can be stabilized over a longer period of time, thus compensating for the heating temperature instability that may be caused by fluctuations in the intensity of solar radiation. This innovative approach is expected to provide a more reliable solution for the application of solar energy in crude oil storage. The solar thermal storage technologies of sensible heat storage [26], latent heat storage (phase change storage) [27,28], and thermochemical energy storage [29] are three important methods for solar thermal utilization and peak shifting [30,31]. Among them, sensible heat storage is the most widely used and has a strong application basis [26,32], but the unit energy storage density of sensible heat storage is slightly insufficient compared with that of phase-change energy storage [33,34]. As such, combination with other heat sources is necessary [35,36] for auxiliary heat supply. At the same time, considering the large amount of low and medium temperature wastewater to be treated within the oil field operation area, the sewage source heat pump is of great significance as an auxiliary heat source for temperature-controlled solar systems of crude oil static storage. This auxiliary heat source can be used to realize multistage recycling of waste heat. This technology not only reduces transportation and handling costs, but also effectively reduces heat loss. There are also a few scholars [37] who introduced the possibility of using a solar- sewage heat pump system for heating, but they did not provide a detailed analysis of its application and influencing factors.

However, it is worth noting that the aforementioned studies mainly focused on the extraction, transportation, and refining processes of crude oil. During static storage of crude oil, conventional natural gas heating or electric heating is still widely used to assist solar energy in maintaining crude oil temperature. Currently, there is relatively little research on using a solar sewage source heat pump system to maintain static crude oil storage temperature; as such, a further exploration and in-depth investigation of its influencing factors are needed. Such research will help reveal the potential for the wider applications of solar energy in the petroleum industry, thereby leading to the advancement of energy efficiency and environmental sustainability.

In this study, a new crude oil temperature maintenance system—the maintenance system of crude oil temperature using dual heat sources with solar synergistic sewage heat pumps (SSHS)—is proposed; in addition, a system simulation model is established based on the TRNSYS platform, and its accuracy is verified through experiments. The annual operating characteristics of the SSHS for large floating top tanks were analyzed with the COP of the sewage source heat pump, the heating demand of the crude oil storage tank, the proportion of crude oil heated using solar energy, the solar collector efficiency, and the crude oil temperature as evaluation indexes. The main objective of the research results is to provide a reference basis for the application of solar thermal utilization technology combined with sewage source heat pump technology in the field of crude oil heating and storage, as well as to provide new ideas for industrial heating, which is of great significance in promoting the green and sustainable development of industrial heating technology.

## 2. Model Description and Numerical Simulation

To clarify the operation mechanism of the SSHS on crude oil heating, a simulation and modeling platform for the SSHS was established, and its physical and mathematical models are described here.

### *2.1. Physical Model*

Based on a $10 \times 10^4$ $m^3$ floating roof oil tank in Daqing, China, a solar phase-change temperature maintenance system was established as an example. Figure 1 shows the physical model of the SSHS.

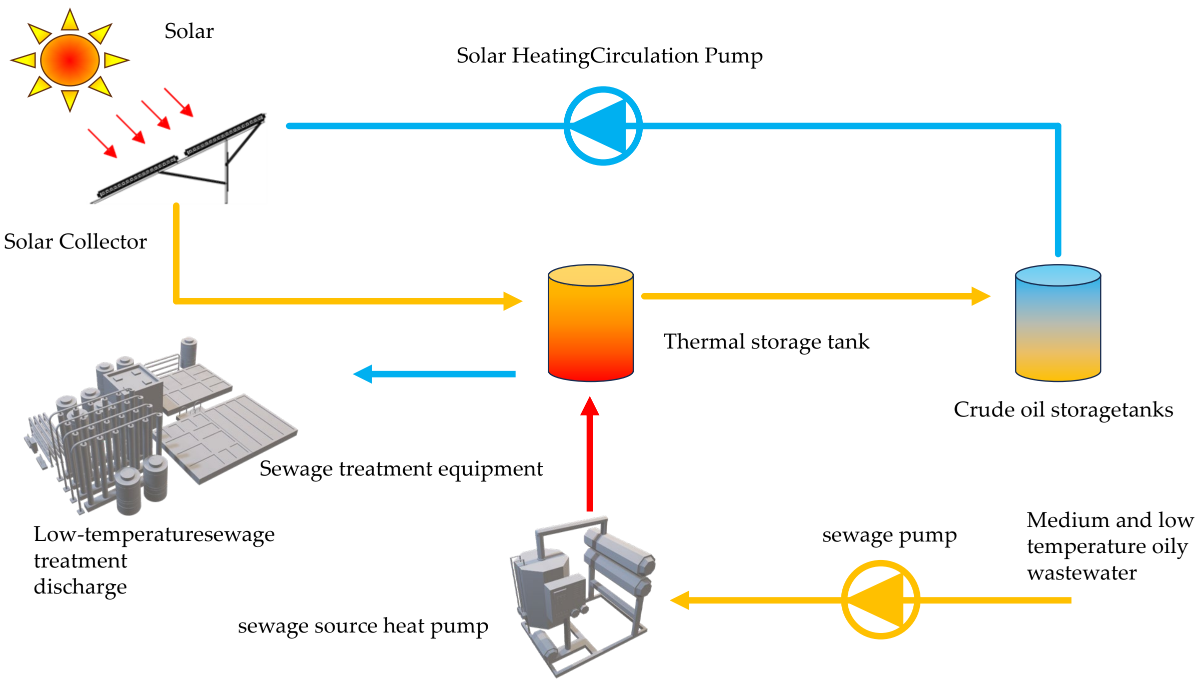


**Figure 1.** Physical model of the SSHS.

The SSHS designed in this study was divided into two main cycle sections: the solar temperature maintenance heating cycle and the sewage-assisted heating cycle. The purpose of the solar temperature maintenance heating cycle is to meet the heating demand of the floating roof tank to maintain the temperature of the static storage crude oil. The main components required for the cycle are solar collectors, sensible heat storage tanks, floating roof tanks, and solar heating circulation pumps. The specific process of the cycle is as follows: the solar radiation absorbed by the solar collector heats the heat transfer medium; the heated heat transfer medium flows into the sensible heat storage tank, where the control system judges whether or not to carry out the heat storage process; the floating top tank enters to heat the crude oil; and this then finally returns to the solar collector for the next cycle. The sewage-assisted heating cycle includes sewage pumps, sewage source heat pumps, and sewage treatment devices. When the heat generated using solar energy cannot meet the heating demand of the crude oil, the sewage source heat pump is turned on to utilize the waste heat of the medium- and low-temperature sewage to heat the crude oil in the floating top tank. This strategy maximizes the ability to ensure that the crude oil temperature is always above its freezing point temperature.

### 2.2. Mathematical Model

#### 2.2.1. Design Parameter Calculation Model

To analyze the system operation characteristics of an SSHS, the following assumptions are proposed [38]: (1) Air is an ideal gas with a constant specific heat. (2) The change in kinetic and potential energy between different components is negligible. (3) Both the heat storage fluid and the heat transfer fluid are incompressible and isotropic. Therefore, based on the above modeling assumptions, the mathematical equation [39,40] of an SSHS for the static storage heating demand of crude oil can be expressed as follows:

$$Q_{oil} = \frac{(K_{wall}A_{wall} + K_{top}A_{top} + K_{bottom}A_{bottom})\Delta T}{1000} \quad (1)$$

where $Q_{oil}$, $K_{wall}$, $K_{top}$, $K_{bottom}$, $A_{wall}$, $A_{top}$, $A_{bottom}$, and $\Delta T$ are the crude oil static storage's thermal load (kW), thermal transfer coefficient of the wall, the top and bottom of the floating roof tank (W/(m·°C)), the area of the wall, the top and bottom of the floating roof tank ($m^2$), and the difference between the temperature of the environment and the maintenance temperature of the crude oil for static storage (°C), respectively.

The thermal transfer coefficient is calculated as follows:

$$K_{top} = \sum \frac{1}{\frac{1}{\alpha_{oil}} + \frac{\delta_i}{\lambda i} + \frac{1}{h_{top}}} \tag{2}$$

$$K_{wall} = \sum \frac{1}{\frac{1}{\alpha_{oil}} + \frac{\delta_i}{\lambda i} + \frac{1}{h_{wall}}} \tag{3}$$

$$K_{bottom} = \sum \frac{1}{\frac{1}{\alpha_{oil}} + \frac{\delta_i}{\lambda i} + \frac{\pi D}{8\lambda_s}} \tag{4}$$

where $\alpha_{oil}$, $\lambda_i$, $\delta_i$, $h_{wall}$, $h_{top}$, $D$, and $\lambda_s$ are the heat transfer coefficient from the crude oil to the storage tanks (W/($m^2$·°C)), the thermal conductivity of I (W/($m^2$·°C)), the thickness of $i$ (m), the convective heat transfer coefficients (W/($m^2$·°C)) for tank walls and tops, the characteristic dimensions of the tank (m), and the thermal conductivity of the soil (W/($m^2$·°C)), respectively.

The convective heat transfer coefficients for the tank walls and tops is calculated as follows:

$$h_{top} = \frac{\lambda_{steel}}{D}\left(0.664\text{Re}^{1/2}\text{Pr}^{1/3}\right) \tag{5}$$

$$h_{wall} = C\frac{\lambda_{baowen}}{D}\text{Re}^{n} \tag{6}$$

where $\lambda_{steel}$, $Re$, $Pr$, $C$, and $\lambda_{baowen}$ are the thermal conductivity of steel (W/($m^2$·°C)), the thickness of i (m), the Reynolds number, the Prandtl number, and the thermal conductivity of the insulation layer (W/($m^2$·°C)), respectively.

The calculated convective heat transfer coefficients for crude oil storage tanks are 1.50 W/$m^2$·°C ($h_{top}$) and 4.57 W/$m^2$·°C ($h_{wall}$).

To ensure the safety of the operation of the large floating roof tanks, the maintenance temperature of crude oil in static storage should be higher than the freezing point temperature of 5–10 °C. After experimental testing, the freezing point temperature of crude oil in the Daqing area was found to be 30.2 °C. The dimensions and parameters, as shown in Table 1, were calculated from measurements and combined with references.

**Table 1.** The dimensions and physical parameters of large floating roof tanks.

| Material | Value |
| --- | --- |
| Diameter of floating roof tank (m) | 80 |
| Height of floating roof tank (m) | 21 |
| Thermal conductivity of wall of floating roof tank (W/(m·°C)) | 0.475 |
| Thermal conductivity of top of floating roof tank (W/(m·°C)) | 1.726 |
| Thermal conductivity of bottom of floating roof tank (W/(m·°C)) | 0.11 |

The solar collector was a vacuum tube collector, and the main design parameter was the heat collection area, which was calculated as follows:

$$A_{solar} = \frac{86,400 Q_{oil} f}{J_T \eta (1-\eta_L)} \tag{7}$$

where $A_{solar}$, $J_T$, $f$, $\eta$, and $\eta_L$ are the collecting area of the vacuum tube collector ($m^2$), the annual average daily solar radiation on the receiving surface of the collector (kJ/$m^2$), the solar guarantee rate, the average collector efficiency, and the solar system average daily loss rate, respectively. The solar guarantee rate is the ratio of the effective heat gain from solar radiation to the required heating demand of a solar collector system during the system design phase.

The sensible heat storage tank is a key component of the SSHS that regulates the cyclical fluctuations of solar energy. The component relies primarily on temperature changes in the material to store and release heat. The volume of the thermal storage tank can be calculated using the following formula:

$$Q_H = \frac{c_{water} m_{water} \Delta t_{water}}{1000} \tag{8}$$

$$V_{water} = \frac{t Q_{oil}}{\rho_{water} Q_H} \tag{9}$$

where $V_{water}$, $t_{water}$, $Q_H$, $\rho_{water}$, $m_{water}$, and $C_{water}$ are the volume of the sensible heat storage tank ($m^3$), the temperature rise of the sensible heat storage tank (°C), the heat storage of the sensible heat storage tank (kJ), the density of the heat storage material ($kg/m^3$), the mass of the heat storage material (kg), and the heat capacity of the heat storage material (J/kg), respectively. In this paper, the calculated volume size was about 300 $m^3$, radius was 4.37 m, and the height was 5 m for the cylindrical tanks with the same material and insulation as the crude oil storage tanks. The principle of regulating the temperature fluctuation of the sensible heat storage tank is mainly through the temperature change in the sensible heat material (e.g., water) inside the tank to realize the regulating effect on the crude oil heating temperature. When the intensity of the solar radiation was large, the excess heat of the collector was stored in the sensible heat storage tank in the form of a temperature rise; when the intensity of the solar radiation was small, the collector heating temperature could not meet the demand, and the sensible heat storage tank, in the form of a temperature drop, saw a release of heat to regulate the fluctuation in temperature.

The formula for calculating the heat loss from the pipe and sensible heat storage tanks is as follows:

$$Q_{storage,loss} = K_{storage} A_{storage} \Delta t_{water} \tag{10}$$

$$Q_{pipe,loss} = K_{pipe} A_{pipe} \Delta t_{HTF} \tag{11}$$

where $Q_{storage,loss}$, $Q_{pipe,loss}$ $K_{storage}$, $K_{pipe}$, $A_{storage}$, $A_{storage}$, $\Delta t_{water}$, and $\Delta t_{HTFr}$ are the heat loss from the pipe and the sensible heat storage tanks (kW), the thermal transfer coefficient of the storage tank and pipe ($W/(m^2 \cdot °C)$), the area of the wall, the top and bottom of the floating roof tank ($m^2$), and the difference between the temperature of the environment and the temperature of the heat transfer fluid (°C), respectively.

The parameters of the crude oil, heat transfer fluid, and water used in this study are shown in Table 2.

**Table 2.** The parameters of the crude oil, heat transfer fluid, and water.

| Material | Crude Oil | Heat Transfer Fluid | Water |
|---|---|---|---|
| Thermal conductivity (W/(m·°C)) | 0.1516 | 2.26 | 0.59 |
| Specific thermal capacity (kJ/(kg·°C)) | 2 | 3.358 | 4.2 |
| Density ($kg/m^3$) | 798 | 1064 | 1000 |

### 2.2.2. Heat Balance Model

The crude oil storage tanks are the ultimate component of the system. Their heat balance equation is the key to our comprehension of the thermal characteristics of the system. The heat balance equation for the tank boundary is as follows:

$$\lambda_{oil}\left(\frac{\partial}{\partial x}\left(\frac{\partial t(x,y)}{\partial x}\right) + \frac{\partial}{\partial y}\left(\frac{\partial t(x,y)}{\partial y}\right)\right) + K_i \frac{\partial (t_i - t(x,y))}{\partial x \partial y} = \rho_{oil} C_{oil} \frac{\partial t(x,y)}{\partial \tau} \tag{12}$$

where $\lambda_{oil}$, $\rho_{oil}$, $C_{oil}$, $K_i$, and $t_i$ are the thermal conductivity (W/(m·°C)), the density ($kg/m^3$) and specific thermal capacity (kJ/(kg·°C)) of the crude oil, the heat transfer coefficient ($W/(m^2 \cdot °C)$) of $i$, and the temperature of the substance with which the crude oil heat is transferred (e.g., environmental temperature, the temperature of the heat transfer fluid, etc.) (°C), respectively.

The boundary conditions are expressed as follows:

$$\alpha_{oil}(t_{top} - t_{oil}) = K_{top}(t_0 - t_{oil}) \tag{13}$$

$$\alpha_{oil}(t_{wall} - t_{oil}) = K_{wall}(t_0 - t_{oil}) \tag{14}$$

$$\alpha_{oil}(t_{bottom} - t_{oil}) = K_{bottom}(t_{soil} - t_{oil}) \tag{15}$$

$$\alpha_{oil}(t_p - t_{oil}) = K_p(t_{HTF} - t_{oil}) \tag{16}$$

where $t_p$, $t_{HTF}$, and $K_p$ are the temperature of (°C) the heat transfer coil, the temperature of the heat transfer fluids, and the heat transfer coefficient (W/(m$^2$·°C)) of the heat transfer coil, respectively.

The initial conditions are expressed as follows:

$$\tau = 0, t(x, y) = t_0 \tag{17}$$

where $t_0$ is the temperature (°C) of the environment.

### 2.3. System Simulation Model Construction

#### 2.3.1. Transient Simulation Model

The SSHS is a heating method that utilizes vacuum tube collectors in conjunction with a sewage source heat pump to heat the HTF (heat transfer fluid) and transfer the heat to the crude oil storage tank. The system consists of a solar collector, a sewage source heat pump, a sensible heat storage tank, a heat pipe network, and a crude oil storage tank. The system simulation built using TRNSYS can further clarify the parameter relationships between the different internal devices. The SSHS simulation model designed in this study is shown in Figure 2.

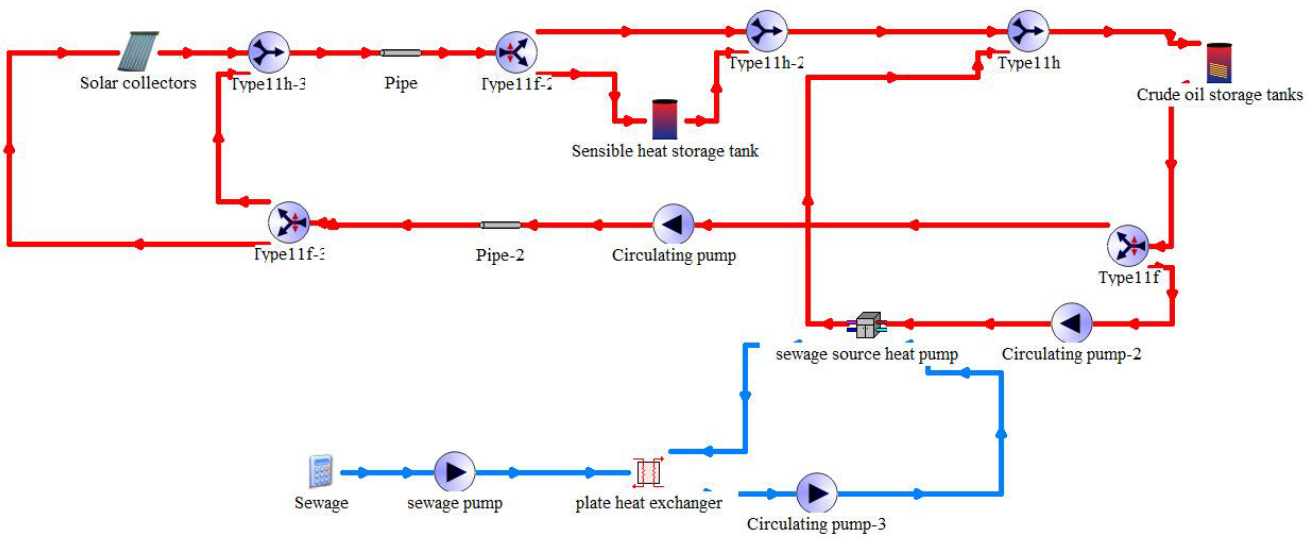


**Figure 2.** Transient simulation model of SSHS.

The SSHS simulation model was built based on TRNSYS 18.0 software. The main components of the SSHS simulation model are as follows: the meteorological parameter module (type 15-2), the vacuum tube collector (type 71), the auxiliary heating equipment (type 659), the crude oil storage tank (type 156), the storage tank (type 158), the circulation water pump (type 114), the plate heat exchanger (type 5), the controller (type 165), the diverter (type 11f), the mixer (type 11h), the sewage source heat pump (type 2256), the graphic output component (type 65c), and the data output component (type 28).

Among them, the solar collector (type 71), sewage source heat pump (type 2256), and circulation water pump (type 114) were found to be the main components of the system. The model and manufacturer of the RTC solar collector was Bailisheng New Energy Technology Co., Shaoxing, Zhejiang, China; the YEWS D-HP water source heat pump was manufactured by YORK Co., PA, USA.; and the water pumps were customized by Changsheng Technology Co., Daqing, China; these are the main parameters that are shown in Tables 3–5.

**Table 3.** RTC solar collector.

| Parameters | Value |
|---|---|
| Combined efficiency (%) | 45 |
| Extreme Output Temperature (°C) | 180 |
| Length (mm) | 3890 |
| Width (mm) | 2950 |
| Height (mm) | 1495 |
| Mounting angle (°) | 55 |

**Table 4.** YEWS D-HP water source heat pump.

| Parameters | Value |
|---|---|
| Rated heat capacity (kW) | 612 |
| Input power (kW) | 173 |
| Evaporator water flow (L/s) | 15.7 |
| Evaporator water pressure drop (kPa) | 16 |
| Evaporator water flow (L/s) | 29.5 |
| Evaporator water pressure drop (kPa) | 37 |

**Table 5.** Customized water pumps.

| Parameters | Collector Heat Circulation Pumps | Condenser Side Water Pump | Evaporator Side Water Pump |
|---|---|---|---|
| Water flow ($m^3$/h) | 306 | 106.2 | 56.52 |
| Water pump lift (m) | 30 | 20 | 20 |
| Combined efficiency | 0.75 | 0.75 | 0.75 |
| Input power (kW) | 35.54 | 8.21 | 4.11 |

### 2.3.2. Validation

Based on the experimental method, the accuracy of the TRNSYS simulation system was verified by heating the crude oil storage tank with a heat storage tank. Figure 3 shows the experimental setup and procedure, and Figure 4 shows the structure and thermocouple (Agilent 34450A, range −80−150 °C, and accuracy 0.002 °C) distribution (ABC(1,2,3), GHJ(1,2,3)) of the crude oil storage tank and heat storage tank. The main equipment used in this verification experiment (the experimental equipment in this study was customized by Changsheng Technology Co., Daqing, China) included a crude oil storage tank, heat storage tank, liquid storage tank, circulating water pump, and electric heating equipment, the dimensions of which are shown in Figure 4. The initial temperature of all three tanks was 10 °C, the power of the electric heating equipment was 6 kW, and the pump flow rate was 1.3 $m^3$/h. The verification experiment process was as follows: First, open the crude oil storage tank bypass valve, the electric heating equipment, and the circulating water pump. Then, heat the heat storage tank to 57 °C and the make-up tank to 70 °C via the electric heating equipment. Subsequently, close the crude oil storage tank bypass valve and electric heating equipment, then use the heat storage tank and make-up tank to heat the crude oil storage tank. Lastly, record its internal temperature change using thermocouples.

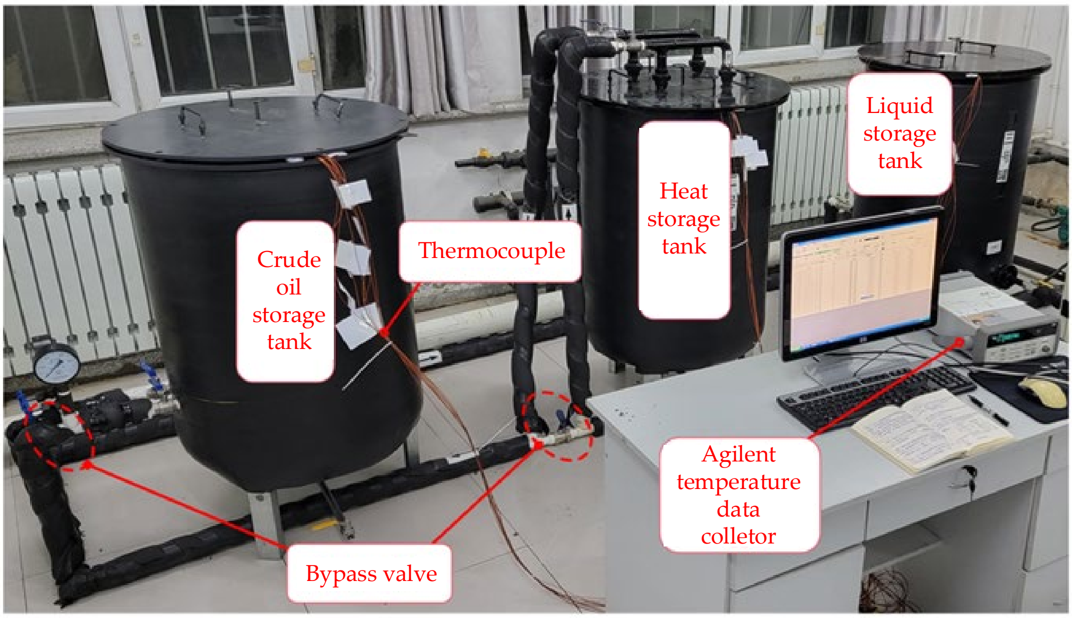


(**a**) Experimental setup

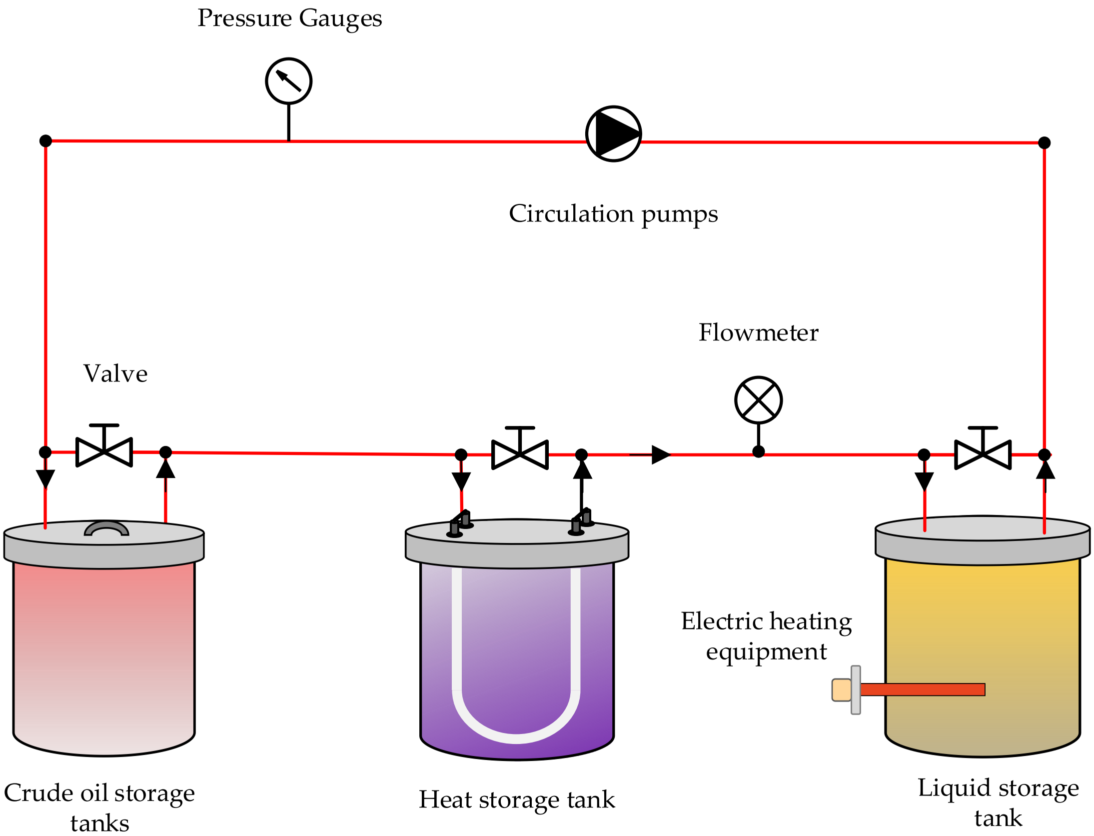


(**b**) Experimental procedure

**Figure 3.** Experimental setup and procedure.

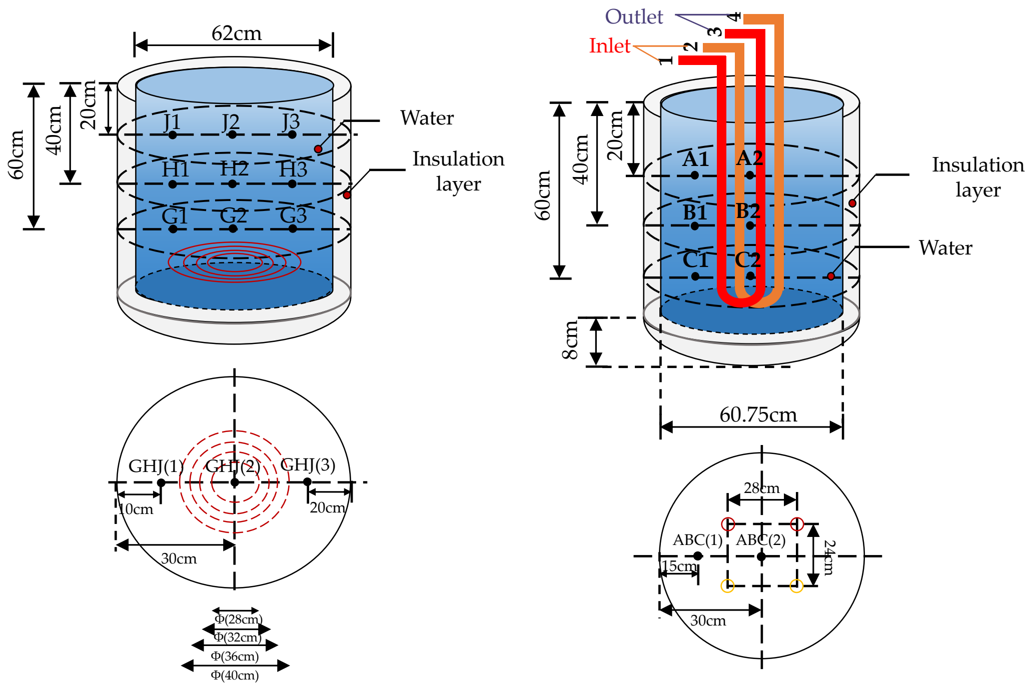


**Figure 4.** The structure and thermocouple distribution of the crude oil storage tank and heat storage tank.

Figure 5 illustrates the trend of the average temperature variation in the crude oil storage tank and heat storage tank. The results showed that the average error in the average temperature of the heat storage tank was 5.6%, and the average error in the average temperature of the floating top tank was 7.39%, which is within the error range [41]. The reason for the error was mainly caused by the accuracy gap between the experimental equipment and the simulation software, as well as the impurities produced by the heat transfer fluid during operation of the equipment. Therefore, the accuracy of the TRNSYS system simulation platform established in this study was acceptable.

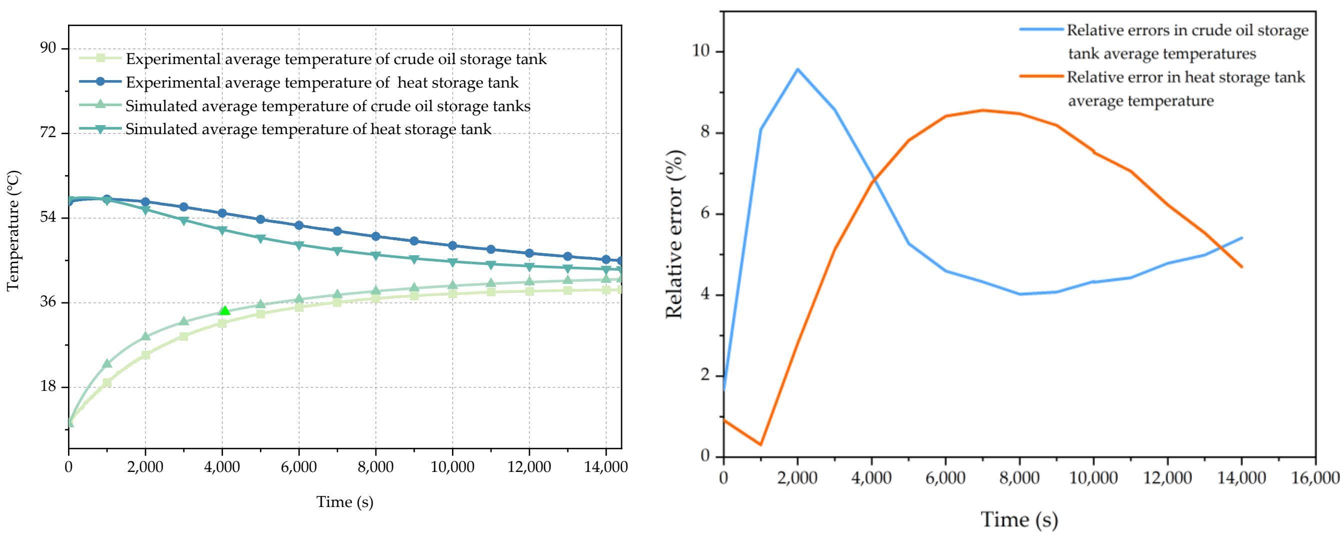


**Figure 5.** Average temperature variation in the crude oil storage tank and heat storage tank.

### 2.4. Performance Parameter Definitions

#### 2.4.1. Proportion of the Crude Oil Heated Using Solar Energy

The proportion of the crude oil heated using solar energy is an important indicator for evaluating the thermal performance of a solar collector and is given by the following:

$$\phi_{solar} = \frac{Q_{solar,s}}{Q_{oil,r}} \times 100\% \quad (18)$$

where $\phi_{solar}$, $Q_{solar,s}$, and $Q_{oil,r}$ are the proportion of crude oil heated by solar energy, the solar heat for crude oil (kJ), and the total heat of the crude oil being heated (kJ), respectively.

#### 2.4.2. Heat Collection Efficiency of the Solar Collectors

The heat collection efficiency of the solar collectors is the ratio of the effective heat collection using the solar collectors to the total solar radiation projected onto the solar collectors, and this can be calculated by the following equation:

$$\eta_{\text{solar}} = \frac{Q_u}{I_u A_c} \quad (19)$$

where $\eta_{\text{solar}}$, $Q_u$, and $I_u$ are the heat collection efficiency of the solar collectors, the effective heat collection using the solar collectors (MJ), and the total solar radiation on the inclined planet (MJ/m$^2$), respectively.

#### 2.4.3. COP for Sewage Source Heat Pumps

The COP is the most important indicator for the evaluation of sewage source heat pumps, and its calculation formula is given as follows:

$$COP = \frac{Q_{sp}}{W_{sp}} \quad (20)$$

where $COP$, $Q_{sp}$, and $W_{sp}$ are the sewage source heat pump coefficient of performance, the heat production (kJ), and the input energy (kJ) of the sewage source heat pumps, respectively.

### 2.5. Meteorological Parameters

The meteorological parameter reading module of the system simulation in this paper used a type15-2 component to read the meteorological data of a typical meteorological year in *.tm2 (the specific file format for weather parameter imports in TRNSYSY), which includes two main parameters: ambient temperature and solar radiation. Figure 6 shows the typical annual meteorological parameters for Daqing, Heilongjiang Province, China (data obtained from the Meteonorm database). From the figures, it can be concluded that the lowest temperature of the year occurs in January with a low of −26.4 °C, whereas the highest temperature occurs in July with a high of 29.4 °C. Solar radiation shows a cyclic variation throughout the year, reaching its maximum in July; the total monthly solar radiation was 300 kWh/m$^2$ for seven months of the year, with a total annual radiation of 3408 kWh/m$^2$.

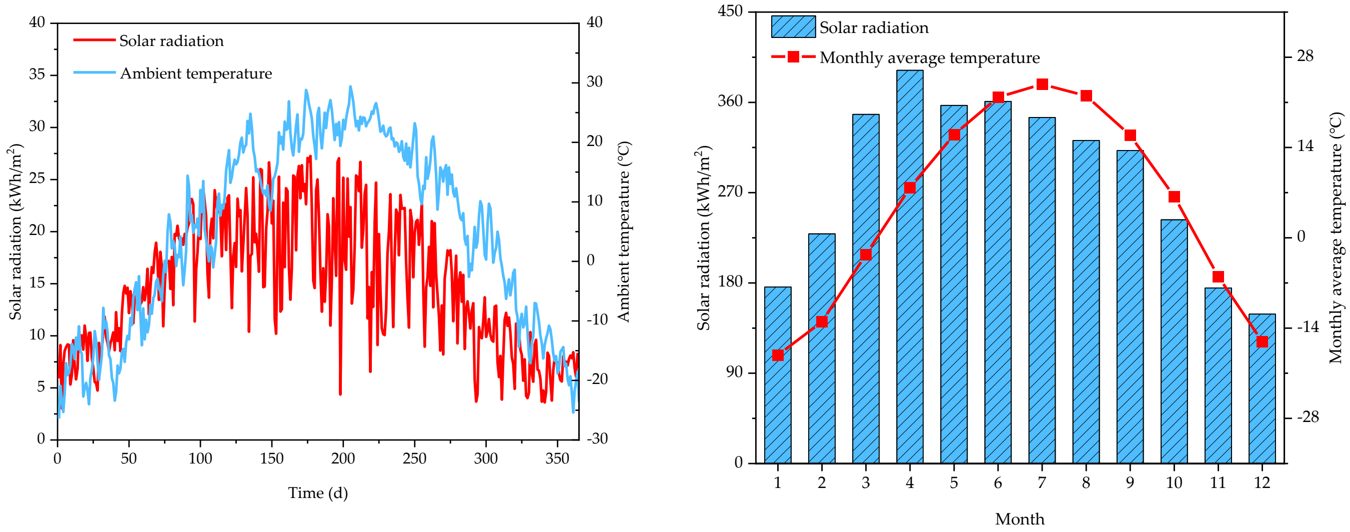


**Figure 6.** Meteorological parameters.

## 3. Results and Discussion

Based on the established simulation model of the SSHS system, the effects of different solar energy guarantee rates, pumping unit flow rates, and effluent supply temperatures on the operational characteristics of the SSHS system were analyzed. The simulation area was set in Daqing, China, and the time period was 1 year with a time step of 1 min.

### *3.1. Effect of Solar Guarantee Rate*

The effect of the solar guarantee rate ($f$) on the thermodynamic properties of solar collectors, crude oil storage tanks, and the performance of sewage source heat pump in the SSHS was evaluated by testing different solar guarantee rates for the SSHS. Different solar guarantee values—namely, 10%, 20%, 30%, 40%, and 50%—were considered, and the results obtained are as follows:

Table 6 presents the calculated collector areas for the different solar guarantee rates based on Equations (1) and (2):

**Table 6.** The collector area at different solar guarantee rates.

| $f$ | $Q_{oil}$ /kW | $A_{solar}$ /m$^2$ |
|---|---|---|
| 10% | 571.24 | 1226.32 |
| 20% | 571.24 | 2452.64 |
| 30% | 571.24 | 3678.95 |
| 40% | 571.24 | 4905.27 |
| 50% | 571.24 | 6131.59 |

To analyze the effect of the solar guarantee rate variation on the thermal collection efficiency of the solar collectors inside the SSHS, five different solar guarantee rates (10%, 20%, 30%, 40%, and 50%) were considered. The obtained solar collector efficiency, proportion of crude oil heated, average annual collector efficiency, and the average proportion of crude oil heated are shown in Figure 7. As expected, in Figure 7a–e, the solar collector's efficiency fluctuated less after the solar collector operation was stabilized. The proportion of the solar heat supply to crude oil rose gradually with the operation of the system. The main reason for this phenomenon is that, in the early stage of system operation, the heat collection capacity of the solar collector is small, and the collector outlet temperature is low, which cannot meet the demand of the static storage of crude oil. In addition, the proportion of heat supply to crude oil from the sewage source heat pump accounts for a larger proportion. With the operation of the system, the cumulative solar heat collection gradually increased, and the proportion of solar energy to crude oil heating also increased. It can also be found that, as the solar energy guarantee rate decreases, the phenomenon of decreasing the proportion of solar energy to crude oil heat supply occurs in the second half of the system operating time. Meanwhile, as shown in Figure 7f, the annual average collector efficiency gradually decreased, and the annual average proportion of the solar heat supply to crude oil also gradually increased, but the magnitude of the increase gradually decreased. This is because, with the increase in solar guarantee rate, the solar collector area increases; as such, the amount of heat collected gradually increases and can meet the demand of crude oil static storage. At the same time, the increase in collector area leads to an increase in collector heat loss, which reduces the collector's efficiency.

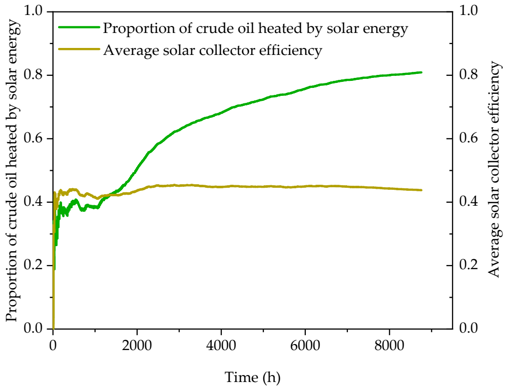


(**a**) A 50% solar guarantee rate

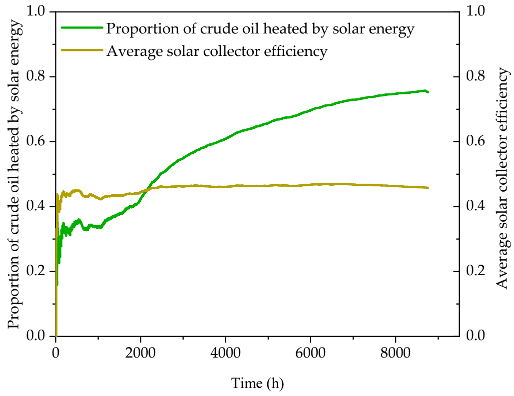


(**b**) A 40% solar guarantee rate

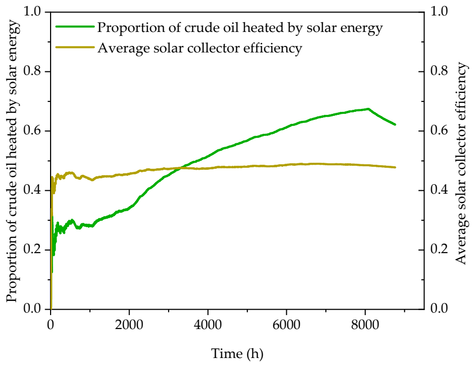


(**c**) A 30% solar guarantee rate

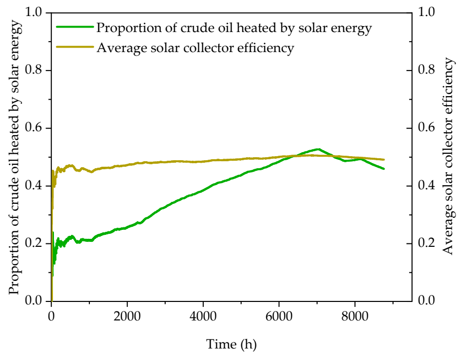


(**d**) A 20% solar guarantee rate

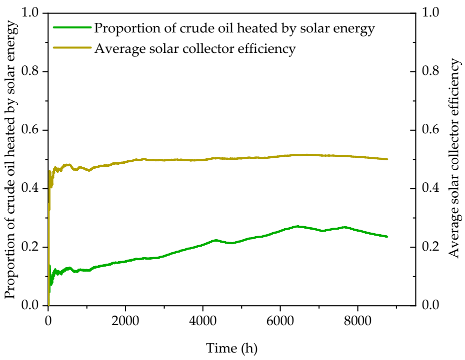


(**e**) A 10% solar guarantee rate

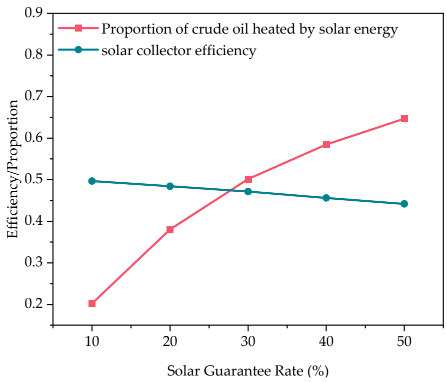


(**f**) The average solar collector efficiency and proportion of crude oil heated

**Figure 7.** Thermal characteristics of solar collectors with different solar guarantee rates.

In order to quantitatively analyze the effect of solar guarantee rates on the crude oil storage tanks, the heating demands of the crude oil storage tanks and the average annual temperature of the crude oil for all the considered scenarios were plotted, as shown in Figure 8a,b. As shown in Figure 8a, with the operation of the system, the heating demand of the crude oil storage tanks shows a trend of decreasing and then increasing, and the heating demand reached its maximum in December at 555,441.75 kWh, 514,226.38 kWh, 500,524.64 kWh, 499,047.9 kWh, and 506,489.14 kWh, respectively. Moreover, it reached its minimum in July at 263,940.78 kWh, 499,047.9 kWh, and 506,489.14 kWh, respectively, at 263,940.78 kWh, 230,099.16 kWh, 193,747.9 kWh, 172,799.63 kWh, and 160,613.90156 kWh (i.e., when the solar energy guarantee was 10%, 20%, 30%, 40%, and 50%), respectively. The main reason for this is that, when the system is working in the summer, the external ambient temperature is high and there is less heat exchange between the crude oil and the environment. However, when working in winter, the external ambient temperature is below zero; as such, the heat exchange between the crude oil and the environment is larger, leading to the phenomenon that the heating demand of the crude oil storage tank is large in winter and small in summer. Combined with Figure 8b, it was found that the average annual temperature of the crude oil increased with an increase in solar guarantee rates, leading to an increase in overall heating demand of the crude oil storage tanks.

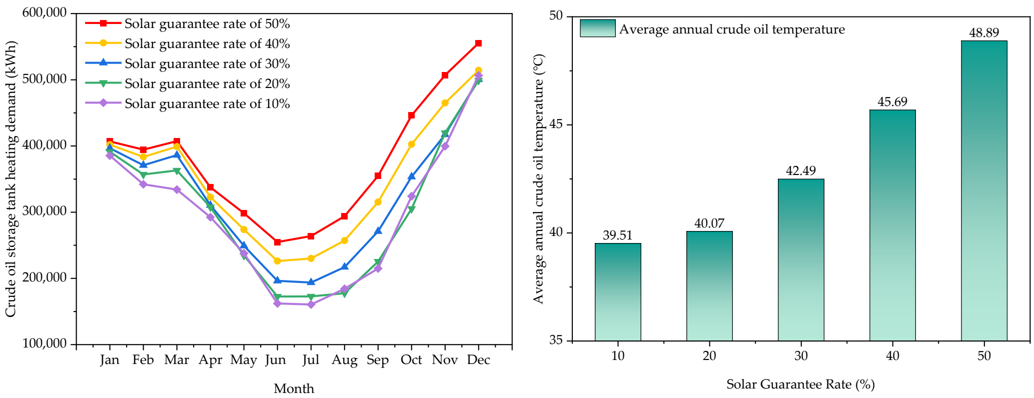


(**a**) Heating demand of crude oil storage tank (**b**) Average crude oil temperature

**Figure 8.** Thermal characteristics of the crude oil storage tank with different solar guarantee rates.

Figure 9a,b plots the hourly COP and average COP of the sewage source heat pump with different solar guarantee rates. As shown in Figure 9, the COP of the sewage source heat gradually decreased as the system operated, and the average COP of the sewage source heat also decreased gradually with the increase in solar guarantee rate. The main reason for this phenomenon was that, with the operation of the system, the cumulative heat collection of the solar collector increased, the temperature of the heat transfer fluid flowing through the condenser end of the sewage source heat pump in the circulation loop gradually increased, and the COP of the sewage source heat pump also decreased. When the solar collector collects heat to meet the crude oil heating demand, the sewage source heat pump is deactivated, at which time, the COP remains unchanged. When the sewage source heat pump is reactivated to meet the crude oil heating requirement (solar energy guarantee rate of 10%, the system operating time > 7000 h), the COP is reduced with the increase in the system temperature of the heat transfer fluid. By the same token, as the solar guarantee rate increased, the temperature of the system loop increased and the COP of the sewage source heat pump decreased. According to Figure 9b, the decrease value in the average COP of the sewage source heat showed a trend of decreasing, then increasing, and then decreasing as the solar guarantee rate changed from 10% to 20%, 20% to 30, 30% to 40%, and 40% to 50%, respectively. In addition, the average COP of the sewage source heat decreased by 0.64%, 0.43%, 1.53%, and 1.33%, respectively.

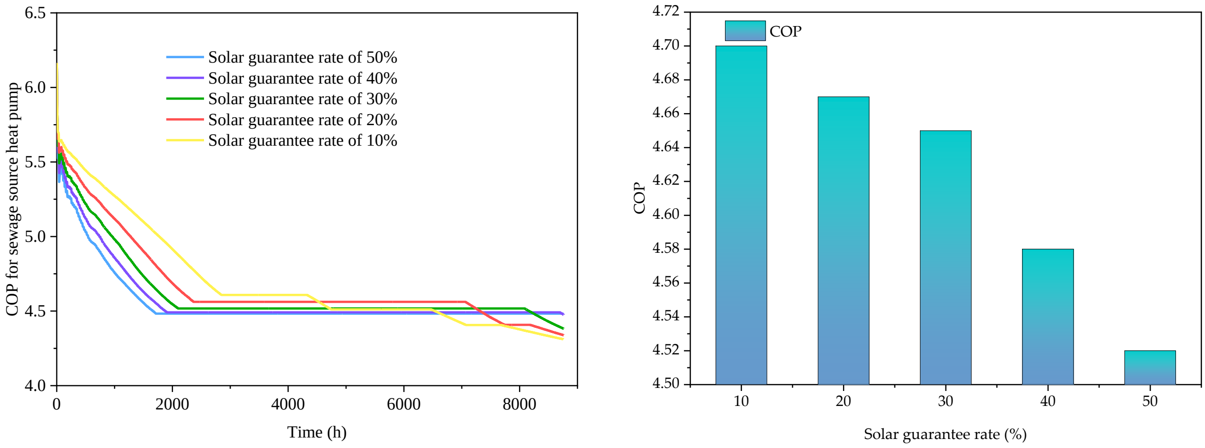


(**a**) COP (**b**) Average COP

**Figure 9.** The thermal characteristics of the sewage source heat pump with different solar guarantee rates.

In summary, the solar guarantee rate should not be too high in order to meet the demand for the heat stored in the crude oil when attempting to maximize solar collector efficiency; furthermore, a solar guarantee rate of 30% is the most appropriate.

### *3.2. Flow Rate of Pumping Units*

As shown in Table 7, the flow rates of five different pump units (heat collecting water pump, sewage pump, and condenser-side water pump form a pump combination, and all three are increased at the same time, with the ratio of their increase being 50:20:25) were selected to study the operating characteristics of the main components of the SSHS when operated at different pump flow rates.

**Table 7.** Different pump flow rates.

| Group | Heat Collecting Water Pump/ $m^3$/h | Sewage Pump/ $m^3$/h | Condenser Side Water Pump/ $m^3$/h |
|---|---|---|---|
| A1 | 80 | 10 | 25 |
| A2 | 130 | 30 | 50 |
| A3 | 180 | 50 | 100 |
| A4 | 230 | 70 | 125 |
| A5 | 280 | 90 | 150 |

Figure 10 details the solar collector efficiency, the proportion of crude oil heated, and the COP of the sewage source heat pump at different pump flow rates with a solar guarantee rate of 30%. As shown in Figure 10a, the solar collector efficiency and the proportion of crude oil heated showed a slight decreasing trend with an increase in the flow rate of pumping units. This is mainly due to the fact that an increase in the flow rate of the collector pump can take away the heat from the collector faster, while an increase in the flow rate of the sewage pump and the condenser-side pump can improve the heat transfer efficiency of the sewage source heat pump. However, when the flow rate of the collector pump is too high, solar radiation cannot be effectively converted into heat, while the flow rate of the sewage pump and condenser-side pump is too high, which also leads to insufficient heat exchange at the hot and cold ends of the sewage source heat pump, which in turn leads to a slight decrease in the amount of heat supplied by the crude oil. The analysis of Figure 10b shows that the COP of the sewage source heat pump demonstrated an increasing trend with the increase in the flow rate of pumping units. For the flow rate of pumping units from A1 to A3, the COP increase was larger, and, from A3 to A5, the COP increase was smaller. For example, when the pumping unit flow rate increased from A1 to A2 and A3, the COP increased by 9.29% and 8.24%, respectively. When the pumping unit flow rate increased from A3 to A4 and A5, the COP increased by 1.11% and 1.09%, respectively. Therefore, considering the economic and equipment constraints, the pumping unit flow rate of A3 was more appropriate.

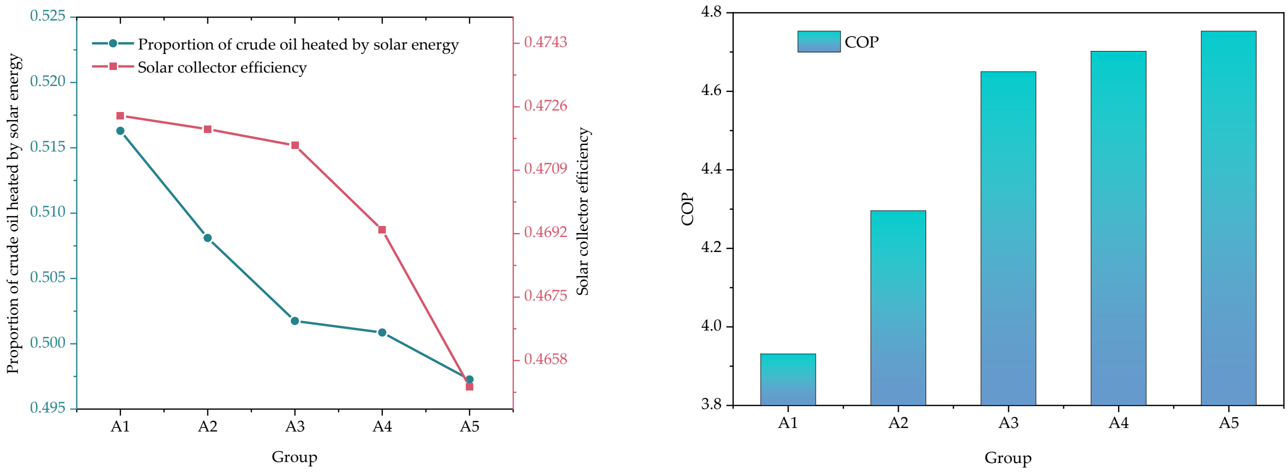


(**a**) Solar collector efficiency and proportion of crude oil heated (**b**) COP

**Figure 10.** The solar collector efficiency, the proportion of crude oil heated and the COP of the sewage source heat pump at different pumping unit flow rates.

### *3.3. Sewage Supply Temperature*

Five different sets of effluent supply temperatures (20 °C, 25 °C, 30 °C, 35 °C, and 40 °C) were selected for simulation to investigate the effect of effluent supply temperature on the operating characteristics of an SSHS under a solar energy guarantee of 30% and a pumping unit flow rate of A3.

The average crude oil temperature, the heating demand of crude oil storage tanks, and the COP of sewage source heat pumps at different sewage supply temperatures are shown in Figure 11. The results show that the average crude oil temperature, the heating demand of crude oil storage tanks, and the COP of sewage source heat pumps gradually increase with an increase in the sewage supply temperature. The main reason for this phenomenon is that when the sewage supply temperature increases, the power required for heating by the sewage source heat pump decreases, and the COP of the sewage source heat pump increases. As such, the temperature of the crude oil supplied by the sewage source heat pump also increases, which leads to an increase in the average temperature of the crude oil and an increase in the heating demand of the crude oil tanks. However, the effect of the sewage supply temperature on the increase in the heating demand of the crude oil tanks was found to be relatively slight; for example, if the temperature of the sewage supply temperature changed from 20 to 40 °C (an increase of 100%), the crude oil storage tank heating demand increase was only 1.43% and the sewage source heat pump COP increased by 9.03%. Therefore, the sewage supply temperature should be increased as much as possible when the conditions allow, which is favorable in terms of improving the COP of the sewage source heat pump.

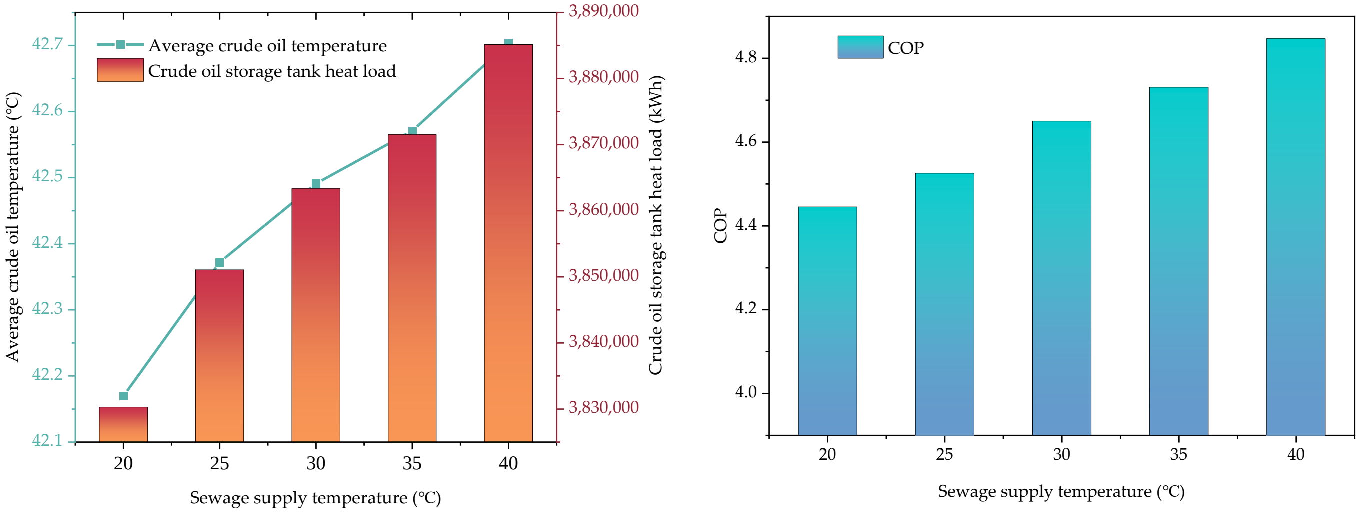


(**a**) Average crude oil temperature and heating demand of crude oil storage tank.

(**b**) COP

**Figure 11.** The average crude oil temperature, the heating demand of the crude oil storage tank, and the COP of the sewage source heat pump at different sewage supply temperatures.

## 4. Conclusions

Dual heat source supply solar sewage source heat pump (SSHS) technology for the static storage of crude oil was proposed to reduce the consumption of primary energy in the heating process of crude oil and to realize green and sustainable development in the field of crude oil temperature maintenance. An SSHS simulation model was developed and experimentally validated. In addition, the operational characteristics of different schemes were compared and analyzed. The relevant research contents and conclusions are as follows:

1. Solar guarantee rate is more important to SSHS; with the increase in solar guarantee rate, the annual average solar collector efficiency gradually decreases, and the annual average proportion of crude oil heated using solar gradually increases. In order to protect the unnecessary waste of heat, the solar guarantee rate should not be too high; in order to meet the demand for heat stored in the crude oil and at the same time maximize the protection of solar collector efficiency, a solar guarantee rate of 30% is most appropriate.
2. The pump unit flow rate has a relatively slight effect on the performance of the solar collector and a large effect on the performance of the sewage source heat pump. With the increase in pump set flow rate, the solar collector's collector efficiency and the proportion of crude oil heated slightly decreased, the COP of the sewage source heat pump showed an increasing trend. For the pump unit flow rate from A1 to A3, the COP increased by a large amount, and from A3 to A5, the COP increased by a small amount. Therefore, considering the economic and equipment limitations, it is more appropriate to use the pumping unit flow rate of A3. At this time, the solar energy guarantee rate is 30%, the pump flow rate is A3, the solar collector efficiency is 50.18%, the proportion of crude oil heated by solar is 47.16%, the average temperature of crude oil is 42.59 °C, and the COP of the wastewater source heat pump is 4.65.
3. The sewage supply temperature has a positive effect on the average crude oil temperature, the crude oil storage tank heating demand, and the COP of the sewage source heat pump. And since the effect of effluent supply temperature on the COP of the sewage source heat pump is much larger than that on the average crude oil temperature and the heating demand of the crude oil storage tank, the performance of the sewage source heat pump can be increased by increasing the sewage supply temperature.

In future work, considering the problems of sensible heat storage such as large volume, the density of heat storage can be enhanced by synergizing the phase change latent heat to further reduce system costs and carbon dioxide emissions and achieve green and sustainable development. Meanwhile, economic studies are needed to assess the feasibility of these practical applications.

**Author Contributions:** Conceptualization, Y.L.; Methodology, S.Z. and X.G.; Formal analysis, M.D.; Investigation, F.Y.; Resources, X.G.; Data curation, S.Z; Writing—original draft, S.Z. and S.L.; Writing review & editing, D.Z. and Y.L; Project administration, Y.L. All authors have read and agreed to the published version of the manuscript.

**Funding:** This research received no external funding.

**Data Availability Statement:** The data presented in this study are available upon request from the corresponding author. The data are not publicly available due to the laboratory interests involved in this data.

**Conflicts of Interest:** The authors declare no conflict of interest.

## Abbreviations

| Abbreviations and Mathematical Symbols | Defined and Described |
|---|---|
| SSHS | Maintenance system of crude oil temperature using dual heat sources with solar synergistic sewage heat pumps |
| SIPH | Solar industrial process heat |
| $Q$ | Thermal load (kW) |
| $K$ | Thermal conductivity (W/(m·°C)) |
| $A$ | Area ($m^2$) |
| $T$ | Temperature (°C) |
| $J$ | Annual average daily solar radiation ($kJ/m^2$) |
| $f$ | Solar guarantee rate |
| $\eta$ | Efficiency |
| $\eta_L$ | Solar system average daily loss rate |
| $V$ | Volume ($m^3$) |
| $\Delta$ | Difference in value |
| $\rho$ | Density ($kg/m^3$) |
| $m$ | Mass (kg) |
| $C$ | Heat capacity (J/kg) |
| $\phi$ | Proportion |
| $COP$ | Coefficient of performance |
| $W$ | Input energy (kJ) |
| $t$ | Temperature (°C) |
| $Re$ | The Reynolds number |
| $Pr$ | The Prandtl number |

## References

1. Chen, J. Oil Reserves: Definition, Calculation, Statistics, and Examples. *Investopedia* **2022**. Available online: https://www.investopedia.com/terms/o/oil-reserves.asp (accessed on 28 July 2022).
2. Ozsarac, V.; Brunesi, E.; Nascimbene, R. Earthquake-induced nonlinear sloshing response of above-ground steel tanks with damped or undamped floating roof. *Soil Dyn. Earthq. Eng.* **2021**, *144*, 106673. [CrossRef]
3. British Petroleum. The Statistical Review of World Energy. *Br. Pet.* **2022**. Available online: https://www.bp.com/de_de/germany/home/presse/nachrichten/statistical-review-of-world-energy-2022.html (accessed on 29 June 2022).
4. Zhao, J.; Dong, H.; Wang, X.; Fu, X. Research on heat transfer characteristic of crude oil during the tubular heating process in the floating roof tank. *Case Stud. Therm. Eng.* **2017**, *10*, 142–153. [CrossRef]
5. Kim, J.S.; Haines, R.J.; Lopez, J.P. A simplified dynamic approach for storage tank thermal inbreathing rates. *Hydrocarb. Process.* **2023**. Available online: https://www.hydrocarbonprocessing.com/magazine/2023/september-2023/tanks-terminals-and-storage/a-simplified-dynamic-approach-for-storage-tank-thermal-inbreathing-rates/#comments (accessed on 15 September 2023).

6. Zhao, J.; Liu, J.; Dong, H.; Zhao, W. Effect of physical properties on the heat transfer characteristics of waxy crude oil during its static cooling process. *Int. J. Heat Mass Transf.* **2019**, *137*, 242–262. [CrossRef]
7. Wang, M.; Zhang, X.; Shao, Q.; Li, J.; Yu, B. Temperature drop and gelatinization characteristics of waxy crude oil in 1000 $m^3$ single and double-plate floating roof oil tanks during storage. *Int. J. Heat Mass Transf.* **2019**, *136*, 457–469. [CrossRef]
8. Ji, S.; Cheng, Q.; Sun, W.; Qi, Y.; Wang, S. Study on optimal operation conditions in the heating process of a crude oil single-disk floating roof tank: Insights from exergy transfer analysis method. *Energy Rep.* **2023**, *9*, 3131–3147. [CrossRef]
9. Sun, W.; Liu, Y.; Li, M.; Cheng, Q.; Zhao, L. Study on heat flow transfer characteristics and main influencing factors of waxy crude oil tank during storage heating process under dynamic thermal conditions. *Energy* **2023**, *269*, 127001. [CrossRef]
10. Mary, E.; Brendan, D. Cold climate air source heat pumps: Industry progress and thermodynamic analysis of market-available residential units. *Renew. Sustain. Energy Rev.* **2023**, *188*, 113739. [CrossRef]
11. Wang, Z.; Shu, L.; Niu, S.; Su, X.; Zhang, S. Research on particle clogging during groundwater recharge of ground source heat pump system. *Geothermics* **2023**, *115*, 102810. [CrossRef]
12. Farjana, S.; Huda, N.; Mahmud, M.; Saidur, R. Solar process heat in industrial systems—A global review. *Renew. Sustain. Energy Rev.* **2018**, *82*, 2270–2286. [CrossRef]
13. Kumar, L.; Hasanuzzaman, M.; Rahim, N. Global advancement of solar thermal energy technologies for industrial process heat and its future prospects: A review. *Energy Convers. Manag.* **2019**, *195*, 885–908. [CrossRef]
14. Nathan, G.; Lee, L.; Ingenhoven, P.; Tian, Z.; Sun, Z.; Chinnici, A.; Jafarian, M.; Ashman, P.; Potter, D.; Saw, W. Pathways to the use of concentrated solar heat for high temperature industrial processes. *Sol. Compass* **2023**, *5*, 100036. [CrossRef]
15. Gil, J.; Topa, A.; Álvarez, J.; Torres, J.; Pérez, M. A review from design to control of solar systems for supplying heat in industrial process applications. *Renew. Sustain. Energy Rev.* **2022**, *163*, 112461. [CrossRef]
16. Mohammadi, K.; Khanmohammadi, S.; Immonen, J.; Powell, K. Techno-economic analysis and environmental benefits of solar industrial process heating based on parabolic trough collectors. *Sustain. Energy Technol. Assess.* **2021**, *47*, 101412. [CrossRef]
17. Hiben, Y.; Bayray, M.; Lauwaert, J. Optimizing solar-assisted industrial heating and cooling system for cost-effective installation. *Appl. Therm. Eng.* **2023**, *230*, 120778. [CrossRef]
18. Kumar, L.; Hasanuzzaman, M.; Rahim, N.; Islam, M. Modeling, simulation and outdoor experimental performance analysis of a solar-assisted process heating system for industrial process heat. *Renew. Energy* **2021**, *164*, 656–673. [CrossRef]
19. Wang, J.; O'Donnell, J.; Brandt, A. Potential solar energy use in the global petroleum sector. *Energy* **2017**, *118*, 884–892. [CrossRef]
20. Halabi, M.; Al-Qattan, A.; Al-Otaibi, A. Application of solar energy in the oil industry—Current status and future prospects. *Renew. Sustain. Energy Rev.* **2015**, *43*, 296–314. [CrossRef]
21. Altayib, K.; Dincer, I. Analysis and assessment of using an integrated solar energy based system in crude oil refinery. *Appl. Therm. Eng.* **2019**, *159*, 113799. [CrossRef]
22. Naseer, A.; Asif, H.; Naveed, A.; Fahid, R.; Mariam, M.; Majid, A.; Kalam, M.; Mujtaba, M. Solar-assisted hybrid oil heating system for heavy refinery products storage. *Case Stud. Therm. Eng.* **2023**, *249*, 103276. [CrossRef]
23. Pathak, S.; Tyagi, V.; Chopra, K.; Kalidasan, B.; Pandey, A.; Goel, V.; Saxena, A.; Ma, Z. Energy, exergy, economic and environmental analyses of solar air heating systems with and without thermal energy storage for sustainable development: A systematic review. *J. Energy Storage* **2023**, *59*, 106521. [CrossRef]
24. Jiang, M.; Feng, G.; Huang, K.; Liu, S.; Liang, D.; Li, H. Research and Analysis of Combined Operational Mode of Solar Energy Hot Water Heating System and Sewage Source Heat Pump Units. *Procedia Eng.* **2015**, *121*, 1544–1555. [CrossRef]
25. Zhang, X.; Wang, E.; Liu, L.; Qi, C.; Zhen, J.; Meng, Y. Analysis of the operation performance of a hybrid solar ground-source heat pump system. *Energy Build.* **2022**, *268*, 112218. [CrossRef]
26. Gautam, A.; Saini, R.P. A review on sensible heat based packed bed solar thermal energy storage system for low temperature applications. *Sol. Energy* **2020**, *207*, 937–956. [CrossRef]
27. Ryu, J.-Y. Alford A, Lewis G, Ding Y, Li Y, Ahmod HK, Park S-H, Park J-P, Branch S, Yu S, Ryu, C. A novel liquid air energy storage system using a combination of sensible and latent heat storage. *Appl. Therm. Eng.* **2022**, *203*, 117890. [CrossRef]
28. Crespo, A.; Barreneche, C.; Ibarra, M.; Platzer, W. Latent thermal energy storage for solar process heat applications at medium-high temperatures—A review. *Sol. Energy* **2019**, *192*, 3–34. [CrossRef]
29. Chen, X.; Wang, F.; Han, Y.; Yu, R.; Cheng, Z. Thermochemical storage analysis of the dry reforming of methane in foam solar reactor. *Energy Convers. Manag.* **2018**, *158*, 489–498. [CrossRef]
30. Chen, H.; Wang, Y.; Li, J.; Cai, B.; Zhang, F.; Lu, T.; Yang, J.; Jiang, L.; Zhang, Y.; Zhou, J. Experimental research on a solar air-source heat pump system with phase change energy storage. *Energy Build.* **2020**, *228*, 110451. [CrossRef]
31. Li, M.Y.; Li, B.; Liu, C.; Su, S.; Xiao, H.; Zhu, C. Design and experimental investigation of a phase change energy storage air-type solar heat pump heating system. *Appl. Therm. Eng.* **2020**, *179*, 115506. [CrossRef]
32. Liu, M.; Riahi, S.; Jacob, R.; Belusko, M.; Bruno, F. Design of sensible and latent heat thermal energy storage systems for concentrated solar power plants: Thermal performance analysis. *Renew. Energy* **2020**, *151*, 1286–1297. [CrossRef]
33. Punniakodi, B.; Senthil, R. Recent developments in nano-enhanced phase change materials for solar thermal storage. *Sol. Energy Mater. Sol. Cells* **2022**, *238*, 111629. [CrossRef]
34. Nazari, M.; Maleki, A.; Assad, M.; Rosen, M.; Haghighi, A.; Sharabaty, H.; Chen, L. A review of nanomaterial incorporated phase change materials for solar thermal energy storage. *Sol. Energy* **2021**, *228*, 725–743. [CrossRef]

35. Ma, Y.; Xi, J.; Cai, J.; Gu, Z. TRNSYS simulation study of the operational energy characteristics of a hot water supply system for the integrated design of solar coupled air source heat pumps. *Chemosphere* **2023**, *338*, 139453. [CrossRef] [PubMed]
36. FScarpa, L.A.; Tagliafico, G. T Integrated solar-assisted heat pumps for water heating coupled to gas burners; control criteria for dynamic operation. *Appl. Therm. Eng.* **2011**, *31*, 59–68. [CrossRef]
37. Qian, J.; Wang, Q. Development on solar—Assisted sewage source heat pump system for crude oil heating. *J. Harbin Univ. Commer. (Nat. Sci. Ed.)* **2017**, *33*, 477–481. [CrossRef]
38. Agrebi, S.; Chargui, R.; Tashtoush, B.; Guizani, A. Comparative performance analysis of a solar assisted heat pump for greenhouse heating in Tunisia. *Int. J. Refrig.* **2021**, *131*, 547–558. [CrossRef]
39. *GB 50495-2019*; Solar Heating Engineering Technical Standard. China Architecture Publishing House: Beijing, China, 2019.
40. *GB 50364-2018*; Civil Building Solar Water Heating System Application Technical Standard. China Architecture Publishing House: Beijing, China, 2018.
41. Li, X.; Qiu, H.; Wang, Z.; Li, J.; Yuan, G.; Guo, X.; Jin, L. Numerical Investigation of a Solar-Heating System with Solar-Tower Receiver and Seasonal Storage in Northern China: Dynamic Performance Assessment and Operation Strategy Analysis. *Energies* **2023**, *16*, 5505. [CrossRef]